AIP Journal of Applied Physics

Photoacoustic characterization of photovoltaic cells

S. M. N. Mello, C. C. Ghizoni, L. C. M. Miranda, and H. Vargas

Citation: Journal of Applied Physics **61**, 5176 (1987); doi: 10.1063/1.338292
View online: http://dx.doi.org/10.1063/1.338292
View Table of Contents: http://scitation.aip.org/content/aip/journal/jap/61/11?ver=pdfcov
Published by the AIP Publishing

Photoacoustic characterization of photovoltaic cells

S. M. N. Mello, C. C. Ghizoni,[a] and L. C. M. Miranda[a]
Instituto de Estudos Avançados, Centro Técnico Aeroespacial, 12200-São José dos Campos, SP, Brazil
H. Vargas
Instituto de Física, Universidade Estadual de Campinas, 13100-Campinas, SP, Brazil

(Received 2 July 1986; accepted for publication 13 January 1987)

The photoacoustic characterization of Si solar-cell samples having distinct internal resistances, both at low and high modulation frequencies, yielded results significantly different from each other. For large samples with very small internal resistances ($\sim 0.1\ \Omega$), the additional contribution of the current dissipation near short-circuit conditions yielded results similar to those obtained with photothermal radiometry or the pyroelectric detection. For small samples, the results for the conversion efficiency, both at low and high modulation frequencies, are similar to ones obtained from the conventional electrical measurements.

The common feature of the photoacoustic (PA) and related photothermal techniques[1,2] is that their signals are proportional to the light into heat conversion efficiency and, therefore, complementary to the other photoinduced energy-conversion processes. This aspect of these techniques has been explored by several authors for investigating photoinduced conversion processes ranging from the study of photosynthetic processes in leaves[3,4] to the monitoring of photovoltaic conversion efficiency of solar cells,[5,6] and the study of nonradiative recombination processes in semiconductors.[7] Since the early works on photoinduced processes using photoacoustics, a few other works using photothermal (or infrared detection) radiometry,[8–10] and pyroelectric detection[11] have appeared in the literature.

In this communication we report on the observations of thermal loss contributions to the photoacoustic characterization of Si solar cells. So far the additional contribution of the internal loss mechanisms to the photothermal characterization of solar cells has been observed only with the photothermal radiometry[10] and pyroelectric[11] detections. The samples used were 4 mm × 4 mm and 2 cm × 1 cm Si solar cells (500 μm thick) from Silicon Sensors. Figure 1 shows the PA-determined photovoltaic conversion efficiency γ as a function of the load resistance R_L for the small sample. The photovoltaic efficiency γ is defined as[2] $\gamma = 1 - S(R_L)/S(\mathrm{OC})$, where $S(\mathrm{OC})$ is the open-circuit PA-signal and $S(R_L)$ is the PA signal at a load resistance R_L. Figures 1(a) and 1(b) show the data recorded at 10 and 200 Hz, respectively, for "white" light front illumination from a 100-W tungsten lamp filtered with a bandpass filter (380 nm $< \lambda <$ 680 nm), whereas Figs. 1(c) and 1(d) correspond to the data taken at 10 and 200 Hz, respectively, for the case of front illumination with a 100-mW argon laser. These data were obtained using a conventional PA chamber with the back contact of the Si cell flushed against the back wall (2-mm glass plate) of the PA chamber. The curves in Fig. 1 show a clear maximum around an optimum load resistance R_L^*; in Fig. 1(a) this maximum occurs at 30 Ω, whereas in Fig. 1(b) it is shifted to roughly 40 Ω. The optimum load resistance as determined from the electrical measurements for the "white" light illumination was around 45 Ω. For the Ar-laser illumination, the optimum load resistance occurred at 15 Ω at 10 Hz [cf. Fig. 1(c)] and at 20 Ω at 200 Hz [Fig. 1(d)]. The electrical measurements yielded an optimum load resistance at 25 Ω for this case of Ar-laser illumination. Thus, we may say that in the case of small sample, the main feature of our PA data for γ is a shift of the optimum load resistance towards the optimum value, given by the electrical measurements, as we increase the modulation frequency.

Figure 2 shows the data for $\gamma(R_L)$ in the case of the large sample. The data were similarly obtained in the pre-

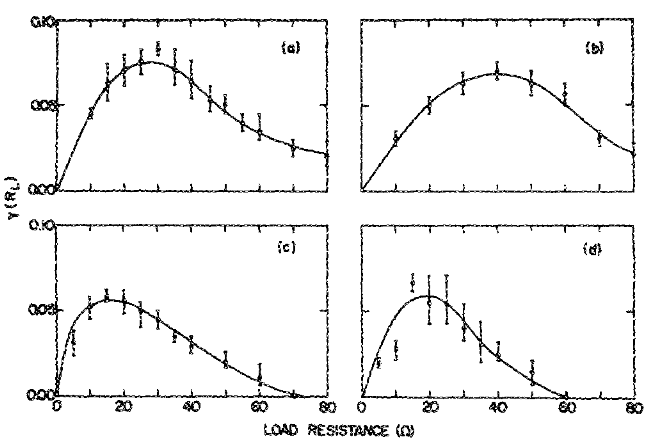

FIG. 1. PA-determined conversion efficiency γ as a function of the load resistance R_L, for a 4 mm × 4 mm, 500 μm thick, Si solar cell under (a) white light illumination at 10 Hz. (b) White light illumination at 200 Hz. (c) 100-mW argon-laser illumination at 10 Hz. (d) 100-mW argon-laser illumination at 200 Hz. The internal resistance R_S, as determined by the dark-current characteristic, is 4.5 Ω and the optimum load resistance, as determined by the electrical measurements, is 45 Ω for the white light illumination and 25 Ω for the argon-laser illumination.

[a] Present address: Laboratório Associado de Sensores e Materiais, Instituto de Pesquisas Espaciais, 12200-São José dos Campos, SP, Brazil.

 0021-8979/87/115176-03$02.40

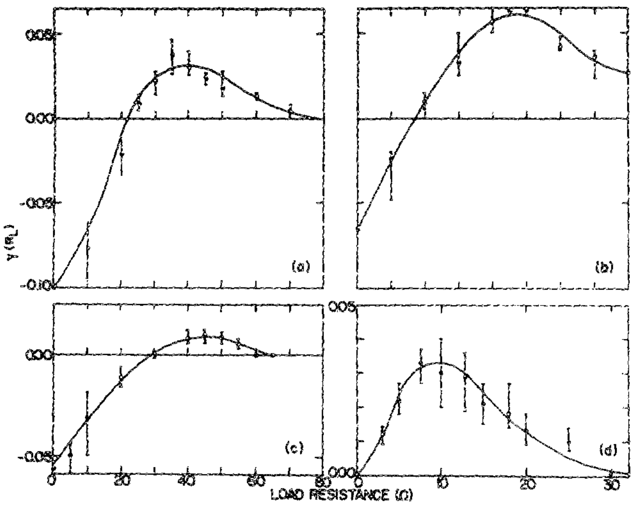

FIG. 2. PA-determined conversion efficiency γ as a function of the load resistance R_L, for a 2 cm × 1 cm, 500 μm thick, Si solar cell under (a) white light illumination at 10 Hz. (b) White light illumination at 200 Hz. (c) 100-mW argon-laser illumination at 10 Hz. (d) 300-mW argon-laser illumination at 140 Hz. The internal resistance determined from the dark-current characteristics is 0.02 Ω. The optimum load resistance determined from the electrical measurements is 50 Ω for the white light illumination, 30 Ω in (c), and 12 Ω in (d).

vious case. The only change is that the back wall of the PA chamber is now the large sample itself. For the "white" light [Figs. 2(a) and 2(b)] as well as for the Ar-laser [Fig. 2(c)] illumination, the curves in Fig. 2 are quite similar to the ones obtained with the pyroelectric detection, as recently reported in Ref. 11, i.e., γ becomes negative for load resistances up to roughly half the optimum load resistance. The fact that γ is negative means that the PA measurement is sensitive to some additional thermal loss mechanisms. As suggested in Ref. 11, this additional thermal loss mechanism is mainly due to the current dissipation at the solar-cell internal resistance. In fact, this suggested mechanism may indeed explain the observed differences, as follows. First, we note that only for small load resistances is the additional heating effective. For a voltage source, it is well known that when the load resistance is matched to the source, half of the generated power is lost in the internal resistance of the source. In the case of the large sample, the fitting of the dark-current characteristics yielded a value of the internal resistance of $R_S = 0.02\,\Omega$. Thus, one would expect that near short-circuit conditions a large amount of heat would be generated in the cell, due to current dissipation. The second argument in favor of this current dissipation mechanism is the modulation frequency dependence of the data of Fig. 2. The Joule heating is mainly generated at the base region (the widest of the three regions) of the solar cell. Furthermore, since the back of the solar cell is a silvered contact, it may be viewed as acting as a heat sink, so that there is a preferential flow, towards this back silvered contact, for the heat generated in the base region. This means that as one increases the modulation frequency (i.e., reducing the thermal diffusion length), the contribution of the Joule heating should get smaller or eventually vanish. This is evidenced in Figs. 2(b) and 2(d) as compared to Figs. 2(a) and 2(c), respectively. In particular, in Fig. 2(d) for the Ar-laser illumination at 140 Hz (for which the thermal diffusion length in Si is of about 440 μm), the thermal loss due to the current dissipation has already disappeared, and the peak of γ occurs at the same load resistance as the one determined by the electrical measurements. To further test this argument, we have next carried out the measurements in the large sample in the PA-transmission configuration; i.e., we have reversed the sample positioning in the PA chamber such that the back silvered contact of the Si cell was inside the PA chamber. The experiment was carried out with white light incident on the front face of the solar cell. In this way we are assured that the detected PA signal is that of heat-transmission configuration, similar to the pyroelectric or ir detections. Figure 3 shows the data for $\gamma(R_L)$ at four different modulation frequencies. At 10 Hz, when the sample is thermally thin, both the photovoltaic and the Joule contributions are present, similar to Figs. 2(a)–2(c). As one increases the modulation frequency, so that we are probing only the heating near the back silvered contact (i.e., near the surface that is in contact with the gas in the PA chamber), the photovoltaic contribution, occurring mainly at the top region of the cell, gets smaller. At modulation frequencies greater than 100 Hz (i.e., thermal diffusion length smaller than approximately 500 μm), only the Joule component is present, as evidenced by the negative value of γ, as a function of R_L. The same PA-transmission type of experiment was attempted with the small sample and no Joule contribution was detected.

In conclusion, we have reported in this communication the observation of additional thermal losses in the PA signal of Si solar cells due to the current dissipation in the internal resistance of the cell. This additional heating occurs at small load resistances when the cell's internal resistance is also small, as in the case of large samples. For small samples the Joule heating due to the current dissipation is very small, producing only a small shift (towards lower values) of the optimum load resistance. For large samples, apart from

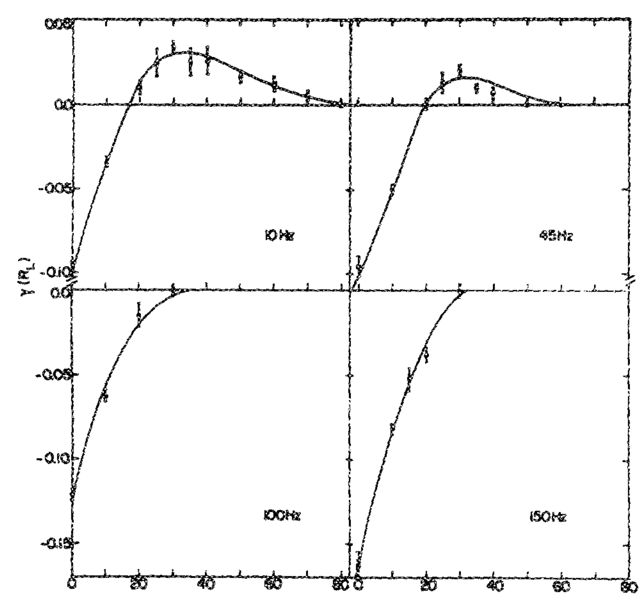

FIG. 3. PA-determined conversion efficiency γ as a function of the load resistance R_L for a 2 cm × 1 cm, 500 μm thick, Si solar cell in the thermal transmission configuration, under white light illumination. The optimum load resistance determined from the electrical measurements is 30 Ω.

shifting the optimum load resistance towards small values, this additional heating also affects the value of the conversion efficiency itself at the optimum load. Since this Joule contribution is generated mainly in the case of the solar cell, its contribution for both small and large samples can be overcome by working at high modulation frequencies.

[1]A. Rosencwaig and A. Gersho, J. Appl. Phys. 47, 64 (1976).
[2]A. Rosencwaig, in *Photoacoustics and Photoacoustic Spectroscopy* (Wiley, New York, 1980).
[3]D. Cahen, S. Malkin, and E. I. Lerner, FEBS Lett. 91, 339 (1978).
[4]C. A. S. Lima, J. C. V. Mattos, A. F. S. Penna, J. F. W. von Bülov, L. C. M. Miranda, and C. C. Ghizoni, J. Photoacoust. 1, 61 (1983).
[5]D. Cahen, Appl. Phys. Lett. 38, 810 (1978).
[6]D. Cahen and S. D. Halle, Appl. Phys. Lett. 46, 446 (1985).
[7]C. C. Ghizoni and L. C. M. Miranda, in *IEEE Ultrasonics Symposium Proceedings*, edited by B. R. McAvoy (IEEE, New York, 1982), Vol. 2, p. 601.
[8]G. Bults, P. E. Nordal, and S. O. Kanstad, Biochim. Biophys. Acta 682, 234 (1982).
[9]S. O. Kanstad, D. Cahen, and S. Malkin, Biochim. Biophys. Acta 722, 182 (1983).
[10]P. E. Nordal and S. O. Kanstad, Infrared Phys. 25, 302 (1985); see also D. Cahen, P. E. Nordal, and S. O. Kanstad, in *4th International Meeting on Photoacoustic, Thermal and Related Sciences Proceedings* (Ecole Polytechnique, Montreal, 1985), paper WD8.
[11]I. F. Faria, Jr., C. C. Ghizoni, L. C. M. Miranda, and H. Vargas, J. Appl. Phys. 59, 3294 (1985).

Barrier height fluctuations in very small devices due to the discreteness of the dopants

D. Arnold and K. Hess
Department of Electrical and Computer Engineering and Coordinated Science Laboratory, University of Illinois at Urbana-Champaign, 1101 West Springfield Avenue, Urbana, Illinois 61801

(Received 22 September 1986; accepted for publication 17 February 1987)

The spatial fluctuation in barrier heights of a planar-doped barrier due to the discreteness of the acceptors and their statistical distribution has been calculated by solving Poisson's equation in three dimensions. Our model assumes a random distribution of spherical acceptor charges. Nonlinear Thomas–Fermi screening has been used to include the effect of free carriers and to determine their position-dependent concentration. At 4.2 K we find a range in barrier heights of 30 meV for a barrier with an average value of 0.206 eV. The method by which potential fluctuations broaden the energy distribution of ballistic electrons is illustrated by an example.

Improvements in lithography and crystal-growth technologies are resulting in increasingly smaller semiconductor device dimensions. As the size of these structures decrease, the role played by statistical fluctuations in the physical parameters of the devices become increasingly important. Since a milestone paper by Schockley in 1961,[1] little work has been reported on quantifying the impact of statistical fluctuations in semiconductor devices with the exception of a study of tunnel diodes by Kane,[2] and work on ohmic contacts by Boudville and McGill.[3]

New device structures are currently considered and fabricated having physical dimensions of the order of 100 Å. Since the average impurity distance is of the same order at a high doping of 10^{18} cm^{-3}, these devices are susceptible to the effects of impurity fluctuations. Significant fluctuation effects have already been identified in problems related to impact ionization,[1] ohmic contacts,[3] and planar-doped barriers.[4]

We concentrate here on the effects pertinent to planar-doped barrier transistors. These structures have been used to deduce the momentum distribution function of high-energy electrons by injecting them over a barrier (emitter) and analyzing them with a second one (collector) after a thin heavily doped drift region (base).[4–6] The barrier height of the collector barrier can be varied with respect to the emitter barrier by changing the applied collector to base voltage. By measuring the collector current as a function of collector barrier height, an estimate of the field directed electron distribution function can be deduced.[5] If the base thickness is of the order of the mean-free path of the electrons then the electrons will drift through the base with few or no scattering events. Such ballistic transport is of interest for high-speed device applications.[4–8]

The current voltage data presented in Refs. 4 and 5 suggest a momentum distribution function which is significantly broader than predicted by Monte Carlo simulations which assumed an ideal, smooth barrier.[9] Fluctuations in barrier height due to spatial variations of acceptor concentration in the barriers have been suggested as the cause of the broadening of the electron distribution function.[4] A tractable formalism has not yet been developed for modeling transport, including dissipation, in a rapidly varying potential; not even in one dimension. Thus, it is presently difficult to accurately calculate the effect of dopant fluctuations on the momentum distribution of electrons traversing a planar-doped barrier. In this communication, however, we present the results of a semiclassical calculation of the barrier height fluctuations. These results give a indication of the upper limit of the effect of dopant fluctuations on the energy distribution of the carriers since quantization will tend to smooth out the fluctuations.

We have solved Poisson's equation in three dimensions